IEEE Access
Multidisciplinary ⋮ Rapid Review ⋮ Open Access Journal

Received April 24, 2019, accepted May 16, 2019. Date of publication xxxx 00, 0000, date of current version xxxx 00, 0000.

Digital Object Identifier 10.1109/ACCESS.2019.2918581

An Uplink UE Group-Based Scheduling Technique for 5G mMTC Systems Over LEO Satellite

OLTJON KODHELI[1], STEFANO ANDRENACCI[2], NICOLA MATURO[1], SYMEON CHATZINOTAS[1], AND FRANK ZIMMER[2]

[1]Snt-Interdisciplinary Centre for Security, Reliability and Trust, University of Luxembourg, 1855 Luxembourg, Luxembourg
[2]SES S.A., 6815 Betzdorf, Luxembourg

Corresponding author: Oltjon Kodheli (oltjon.kodheli@uni.lu)

This work was supported by the Luxembourg National Research Fund (FNR) under Industrial Fellowship Scheme with industrial partner SES S.A., project title "Communication algorithms for end-to-end satellite-IoT (SATIOT)", grant FNR12526592.

ABSTRACT Narrowband Internet of Things (NB-IoT) is one of the most promising IoT technology to support the massive machine-type communication (mMTC) scenarios of the fifth generation mobile communication (5G). While the aim of this technology is to provide global coverage to the low-cost IoT devices distributed all over the globe, the vital role of satellites to complement and extend the terrestrial IoT network in remote or under-served areas has been recognized. In the context of having the global IoT networks, low earth (LEO) orbits would be beneficial due to their smaller propagation signal loss, which for the low complexity, low power, and cheap IoT devices is of utmost importance to close the link-budget. However, while this would lessen the problem of large delay and signal loss in the geostationary (GEO) orbit, it would come up with increased Doppler effects. In this paper, we propose an uplink scheduling technique for a LEO satellite-based mMTC-NB-IoT system, able to mitigate the level of the differential Doppler down to a value tolerable by the IoT devices. The performance of the proposed strategy is validated through numerical simulations and the achievable data rates of the considered scenario are shown, in order to emphasize the limitations of such systems coming from the presence of a satellite channel.

INDEX TERMS 5G, mMTC, NB-IoT, LEO satellite, scheduling technique, differential Doppler shift.

I. INTRODUCTION

In the last years, there has been an ever growing industrial and scientific interest in the Internet of Things (IoT) technology, motivated by the potential of these systems to satisfy important market segments through a very wide variety of use cases and applications with different Quality-of-Service (QoS) requirements. Over time, IoT is expected to have a significant impact and play a key role in the global economic processes and the quality of every-day life [1]–[3]. Based on the nature of the deployed application, IoT can be segmented into massive and critical IoT, with very distinguishable network requirements [4]. Massive IoT consist of billions of devices spread throughout the globe able to generate and report information to the cloud on a regular basis, such as sensors in a smart home or smart city, monitoring devices in smart metering etc. These devices must be low cost and guarantee a very long battery life (up to 10 years) connected through a delay tolerant network. On the other hand, critical IoT has to do with ultra-high reliability and extremely low latency communications with applications such as remote surgery, health care, tactile Internet, traffic safety, vehicular control systems etc [5]. The fifth generation of mobile radio communication systems (5G) introduced two new use cases, besides the traditional mobile broadband (MBB) services, the massive machine type communication (mMTC) for massive IoT and ultra reliable and low latency communication (uRLLC) for critical IoT, as specified by the International Telecommunications Union-Radio (ITU-R) [6]. In order to align with the above-mentioned requirements of massive IoT, the 3rd Generation Partnership Project (3GPP) set up the Narrowband (NB)-IoT and Long-Term Evolution (LTE)-M standard as part of Release 13 [7]. Even though they are widely known as 4G technology, due to the compatibility within the LTE network, they will play a vital role in the 5G systems as well. As a matter of fact, 3GPP has agreed that the mMTC services will be accommodated by further evolving NB-IoT and LTE-M as part of the 5G specifications and no

The associate editor coordinating the review of this manuscript and approving it for publication was Mahmoud Barhamgi.

new standard will be considered in the foreseeable future [8]. To this aim, 3GPP has currently started a work item in the 5G core network to support LTE-M and NB-IoT radio access networks, to ensure a smooth transition of these technologies into 5G [9]. Both are also known as cellular IoT since they are part of a cellular network. Other appealing non-cellular IoT technologies worth mentioning here, for providing low-power and long-range communications, are LoRa [10] and SigFox [11]. However, in the paper, we will only focus the study on the 5G cellular IoT.

The essential challenge of massive IoT networks, with regard to connectivity, is to ensure global and ubiquitous coverage to the IoT devices. Nevertheless, in various cases, these devices are distributed in remote areas (e.g. desert, ocean, forest, etc.) where the terrestrial network does not exist or it is too impractical/cost-ineffective to reach. Moreover, terrestrial networks are still, not capable of connecting the enormous number of IoT devices and terminals deployed all over the world. As a result, the role of the satellite to extend and complement the terrestrial IoT network is crucial and irreplaceable. Indeed, 3GPP started the new radio access network (RAN) activities related to Non-Terrestrial Networks, which aims to study the feasibility of integrating and deploying the satellite access into the 5G network [12]. In this preliminary work, two use cases were analyzed, mMTC and enhanced mobile broadband (eMBB), and the challenges of integrating a satellite access network with different orbital architecture, e.g. geostationary orbit (GEO), medium earth orbit (MEO) and low earth orbit (LEO) have been identified. In addition to the 3GPP standardization effort, many contributions in the literature address satellite-based mMTC networks. Authors in [13], [14] study the key aspects and the role of the satellites in the 5G mMTC communications. Moreover, in [15] a new radio interface is proposed, suitable for MTC services over GEO satellites, while in [16] new random access schemes applicable to satellite networks for machine type traffic were treated. A survey on satellite-based wireless sensor networks, focusing on system architectures and scenarios using different orbits (GEO, MEO, LEO) can be found in [17].

In the above context of having global IoT networks, LEO orbits would be beneficial due to their smaller delay and propagation signal loss, which for the low complexity, low power and cheap IoT devices is of utmost importance to close the link-budget, as shown in [18]–[21]. However, while this would lessen the problem of large delays in the GEO orbit, it would also result in an increased Doppler shift. This particular physical phenomenon arises as a result of the high-speed movement of the LEO satellite with respect to the users on Earth. The Doppler shift can be subdivided into two contributors: the mutual Doppler shift experienced at a reference point or user in the satellite spotbeam (e.g., the center of a spotbeam), and the differential Doppler shift resulting from the location variation of the users inside the spotbeam, communicating with the satellite at different elevation angle. Both problems have been identified in the 3GPP community [22], as well as in the literature [23]. You You *et al.* [24] propose an adaptive Doppler compensation scheme using location information of a user terminal and satellite, along with a weighting factor for the reduction of prediction error. Moreover, in [25] and [26] GNSS based solutions for satellite position estimation and Doppler shift compensation in LTE/5G over a LEO mega-constellation are suggested. In the same way, in [27] a Doppler estimator is proposed, combining the predictable Doppler characterization of the circular LEO orbit with the structure of the cyclic prefix (CP) in orthogonal frequency division multiplexing (OFDM) systems. Other estimators that exploit the redundancy introduced in the CP for Doppler shift compensation of OFDM are presented in [28] and [29] and promising results in additive white Gaussian noise (AWGN) channels are shown. All the above-mentioned techniques are able to mitigate the mutual Doppler shift, if applied in the gateway, and the differential Doppler shift, if applied in the user side. Nevertheless, while at the gateway we have enough power to afford raised complexity of the algorithms, the same does not hold for the users. Indeed, adding extra algorithms at the user side for differential Doppler compensation means moving further away from the IoT vision of very cheap and low complexity devices. As a matter of fact, alternative solutions should be found to keep the same complexity of the users as in the terrestrial IoT network.

Extending the work in [31], in this paper we come up with an uplink scheduling technique for a LEO satellite-based mMTC-NB-IoT system, able to mitigate the level of the differential Doppler down to a value tolerable by the IoT devices, as specified in the standard. The performance of the proposed strategy is validated through numerical simulations of an end-to-end NB-IoT over satellite communication system, focusing only on the uplink case. In addition, we go one step further and show the achievable data rates of the considered scenario, in order to stress out the boundaries and limitations of such systems coming from the presence of a satellite channel. The main contributions of this work relative to the recent literature in the field, are summarized as follows:

- The proposed technique does not increase the complexity at the user side, hence no modifications are needed for the NB-IoT devices. This assures seamless connectivity and service to the devices, regardless of the presence of a satellite or a terrestrial network, aligning with the aim of having an integrated satellite-terrestrial network.
- Even though the Doppler effects occur in the physical layer (PHY) of communication, we address the differential Doppler through a medium access control (MAC) layer approach.
- Despite tha fact that we formulate the problem and validate the techniques using a satellite-based NB-IoT system, the proposed techniques to reduce the differential Doppler shift are applicable to other 5G mMTC applications, such as LTE-M, with only small adaptations.

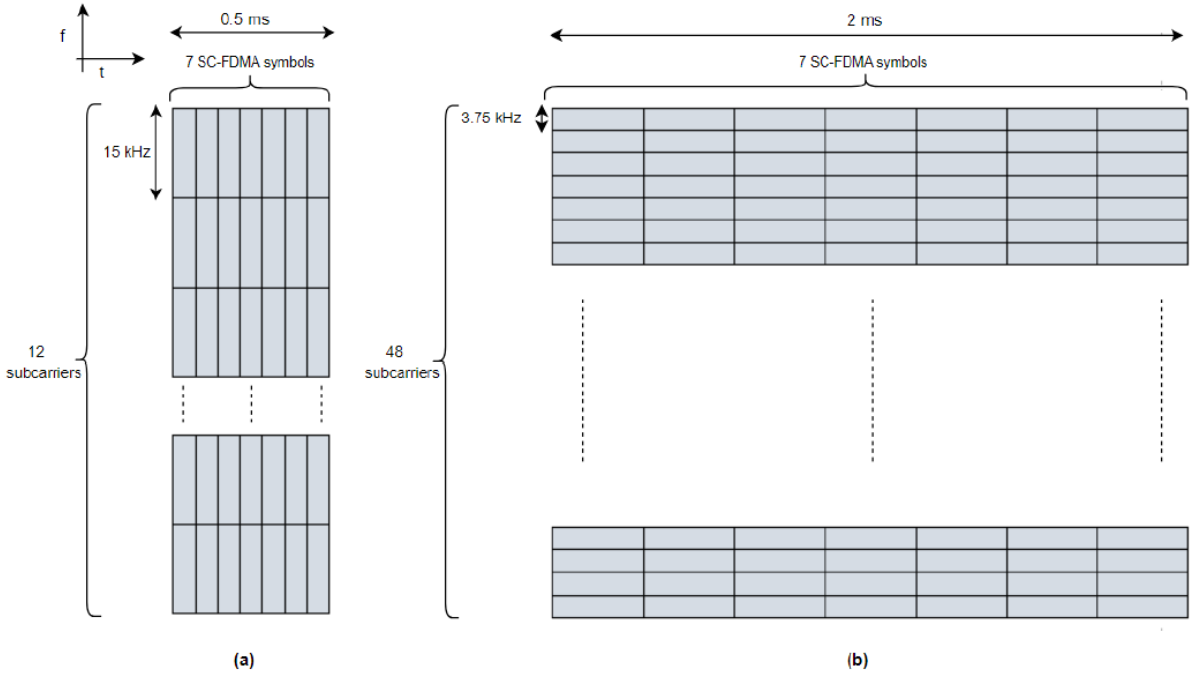

FIGURE 1. Slot structure with (a) 15 kHz SCS for both DL and UL; (b) 3.75 kHz SCS only for UL [30].

The remainder of this paper is organized as follows. Section II provides a brief overview of the user equipment (UE) procedures and the PHY channels involved in the uplink scheduling and time-frequency resource assignment in the NB-IoT. In Section III, the system architecture and the signal model are outlined. In Section IV the differential Doppler problem is formulated, followed by the proposed solution in section V. Section VI and VII yield the simulation results of our scenario, which validate the proposed solutions and evaluate the achievable data rates as a function of satellite elevation angle. Finally, Section VIII concludes the work and highlights the future work.

II. A BRIEF OVERVIEW OF UPLINK SCHEDULING IN NB-IOT

The main aim of this section is to explain the procedures and signaling involved in the uplink scheduling of users and time-frequency resource assignment. To this aim, the reader will be firstly introduced to a general description of the downlink and uplink resource structure and two main NB-IoT PHY channels, Narrowband Physical Downlink Control Channel (NPDCCH) and Narrowband Physical Uplink Shared Channel (NPUSCH). The former is responsible for carrying the necessary control information for scheduling, both downlink and uplink, while the latter carries the uplink data to be transmitted from the NB-IoT devices to the base station (eNB). The information provided in this section, will then be used to design the scheduler for NPUSCH channel and to test its performance over a satellite link in section VI. Appropriate references are provided, mostly coming from 3GPP Specifications (Release 14 and 15) [32]–[34] of NB-IoT, for interested readers to obtain much more detailed information.

A. TIME-FREQUENCY RESOURCE STRUCTURE

In the downlink, orthogonal frequency division multiple access (OFDMA) is applied with a subcarrier spacing (SCS) of 15 kHz. One OFDM symbol contains 12 subcarriers occupying this way the whole NB-IoT bandwidth of 180 kHz. It is important to stress out here that this bandwidth corresponds to one physical resource block (PRB) of the LTE, in order to make NB-IoT operational in the LTE bandwidth. Based on where the NB-IoT carrier is placed in the LTE bandwidth, there are 3 modes of operation: in-band, guard-band and stand-alone. Seven consecutive OFDM symbols form one slot and by summing them up, the subframes and radio frames are formed in the same way as in LTE. The total duration of one slot corresponds to 0.5 ms and two consecutive slots form one subframe. In addition, 10 consecutive subframes compose a radio frame of 10 ms. In the uplink, single-carrier frequency division multiple access (SC-FDMA) signal is used. A discrete Fourier transform (DFT) is applied to the complex modulated data, before mapping them into subcarriers. These data can be binary phase shift keying (BPSK) or quadrature phase shift keying (QPSK) modulated depending on the PHY uplink channel. There exist two SCS options for the uplink transmission (15 kHz and 3.75 kHz), and the corresponding resource grid for each of them is shown in Figure 1. Please note that, for the 15 kHz subcarrier spacing, the slot structure (slot duration in time domain and number of subcarriers) is the same as in the downlink case. Whereas, for the 3.75 kHz subcarrier spacing, the SC-FDMA symbol duration is four

times larger. Therefore, the duration of a slot consisting of seven SC-FDMA symbols is 2 ms, compared with 0.5 ms in the case of 15 kHz subcarrier spacing. Furthermore, the total number of subcarriers in the frequency domain is also four times as large i.e. 48, thereby occupying the same 180 kHz as in the case of 15 kHz subcarrier spacing.

B. NPDCCH AND NPUSCH FEATURES

NPDCCH channel carries the Downlink Control Information (DCI) regarding the downlink and uplink scheduling and resource allocation, acknowledgement or non-acknowledgement (ACK/NACK) information for the uplink transmissions, paging information and uplink resource grant. There are three DCI formats defined and each of them is responsible for delivering different information: DCI format N0 used for uplink scheduling and ACK/NACK feedback on uplink transmissions, DCI format N1 used for downlink scheduling and DCI format N2 used for conveying paging information.

TABLE 1. NPUSCH resource unit definition [34].

SCS	Nr. of tones	SC-FDMA symbols	TTI	Nr. of slots
15 kHz	12	14	1 ms	2
	6	28	2 ms	4
	3	56	4 ms	8
	1	112	8 ms	16
3.75 kHz	1	112	32 ms	16

NPUSCH channel carries both, data and control information coming from the UEs. The distinction between them is done by using two different formats. While format 1 is used for sending dedicated uplink data from the UE to the eNB, format 2 is used for signaling hybrid automatic repeat request (HARQ) acknowledgement for downlink data. NPUSCH supports single-tone transmission and multi-tone transmission. In the single-tone transmission, both SCS options can be used (3.75 or 15), whereas the multi-tone transmission (3, 6, 12 tones) uses SC-FDMA with 15 kHz SCS. Based on the number of tones used, the NPUSCH will have different resource unit representation in the time-frequency domain (refer to Table 1). Please note that the resource unit (RU) is the smallest schedulable element in the uplink transmission. As one can see, assigning fewer resources in the frequency domain (fewer subcarriers), will correspond to a longer transmission time interval (TTI) for the NPUSCH channel. In order to extend coverage and capacity, an important feature of NPUSCH is the support of different modulation and coding schemes (MCS) and time-domain repetition. Mapping different TBS size into a specific RU provides different Turbo code gains, which then will be able to support different coverage levels. The same holds for time-domain repetition of the channel. When the repetition is enabled, it helps to improve the coverage, since the same channel is sent more than once and consequently increasing the SNR. The available TBS sizes for NB-IoT corresponding to different MCS are summarized in Table 2. For multi-tone transmission mode, only QPSK modulation is used and I_{TBS} corresponds to MCS level. Whereas for single-tone transmission BPSK is used only for I_{TBS} 0 and 2. It can be noted that for single-tone transmission, the two last MCS levels (11, 12) are not reachable [33].

TABLE 2. Transport block size (TBS) table for NPUSCH [34].

I_{TBS}	I_{RU}							
	0	1	2	3	4	5	6	7
0	16	32	56	88	120	152	208	256
1	24	56	88	144	176	208	256	344
2	32	72	144	176	208	256	328	424
3	40	104	176	208	256	328	440	568
4	56	120	208	256	328	408	552	680
5	72	144	224	328	424	504	680	872
6	88	176	256	392	504	600	808	1000
7	104	224	328	472	584	712	1000	
8	120	256	392	536	680	808		
9	136	296	456	616	776	936		
10	144	328	504	680	872	1000		
11	176	376	584	776	1000			
12	208	440	680	1000				

C. UE PROCEDURES FOR NPUSCH SCHEDULING

After reception of the NPDCCH with DCI format N0, the UE would have all the necessary information to schedule its NPUSCH containing the uplink data to send towards the eNB. Some of the most important parameters contained in the DCI are shown in Table 3. Basically, these parameters will determine the time-frequency resources and transmission duration for each UE that has uplink data to transmit. There are 12 subcarriers in the frequency domain and 4 different scheduling delay options in the time domain. Specifically, the 2 bit I_{Delay} field in the DCI format N0 signal determines the beginning of the NPUSCH transmission in subframe $n + k_0$. In this case, n is the last subframe of NPDCCH and k_0 is the number of subframes the UE has to wait before starting the uplink transmission. This allows to the UE an ample NPDCCH channel decoding time. Furthermore, after reading the N_{RU} and N_{Rep} field of the DCI the UE will know how long the transmission will last. Regarding the frequency resources, the UE will be provided with the transmission mode (single or multi-tone) and with the subcarriers it should use to modulate the data, in the I_{SC} field. Last but not least, apart from the time-frequency resources, information regarding the modulation order and MCS to use will be assured. This is realized by the I_{TBS} field and I_Q field (1 for BPSK and 2 for QPSK). Overall, the UE will have a corresponding NPUSCH transmission using NPUSCH format 1 in N consecutive NB-IoT UL slots according to the NPDCCH information where $N = N_{Rep}N_{RU}N_{slots}^{UL}$. Note that N_{slots}^{UL} depends on the number of tones used for transmission (see Table 1). After completing the NPUSCH transmission, the UE monitors NPDCCH to discover whether NPUSCH is received correctly by the eNB, or a retransmission is needed. Figure 2 shows an example of how different users can be scheduled in the same radio frame. To conclude, together with the MCS selection, uplink power control is also an important

TABLE 3. Parameters in the NPDCCH DCI Format 0 for NPUSCH Scheduling [34].

Scheduling Delay		Allocated SC		Number of RU		Number of Rep	
I_{Delay}	k_0	I_{sc}	n_{sc}	I_{RU}	N_{RU}	I_{Rep}	N_{Rep}
0	8	0-11	I_{sc}	0	1	0	1
1	16	12-15	$3(I_{sc}$-12) + {0,1,2}	1	2	1	2
2	32	16-17	$6(I_{sc}$-16) + {0,1,2,3,4,5}	2	3	2	4
3	64	18	{0,1,2,3,4,5,7,8,9,10,11}	3	4	3	8
		19-63	Reserved	4	5	4	16
				5	6	5	34
				6	8	6	64
				7	10	7	128

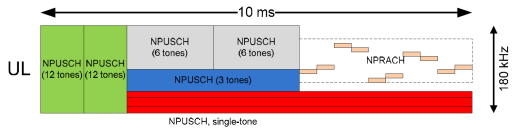

FIGURE 2. Example of NPUSCH scheduling in 10 ms radio frame [35].

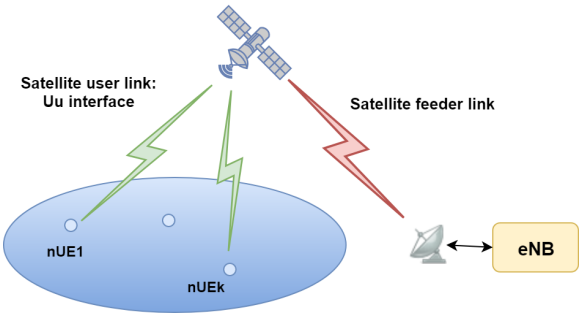

FIGURE 3. NB-IoT over LEO satellite moving over the coverage area.

aspect worth mentioning here. It controls the transmit power of the different NPUSCCH channels, based on the channel quality of the users. Since the channel quality indicator (CQI) reporting from the UE is not supported in NB-IoT, the scheduler relies on the ACK/NACK feedback which a UE provides, for power assignment in the uplink [34].

III. OUR SYSTEM MODEL

In this section, we will describe the system architecture under consideration and provide the systems parameters and assumptions. Furthermore, the mathematical representation of the signal model will be given, for the downlink as well as for the uplink transmission.

A. ARCHITECTURE AND SYSTEM PARAMETERS

In our scenario, we consider a direct access network from the IoT devices (UE) to the base station (eNB), provided by the LEO satellite link. This architecture option is already identified in the 3GPP Technical Specification [12], studying the NR to support non-terrestrial network (NTN). The targeted coverage area has a diameter $D = 200$ km where the UEs are placed (please refer to Figure 3). The amount of time the coverage area will be satisfied with service, depends on the altitude of the satellite, the minimum elevation angle of communication and the directivity of the antenna. The satellite we take into account is a LEO satellite with an altitude $h = 1000$ km and a minimum elevation angle of communication $\alpha_{min} = 45$ degrees. In addition, the following assumptions are made for our satellite-based NB-IoT system: *i*) the channel between the eNB and the satellite (feeder link) as ideal. This assumption is justified by the scope of the study, which focuses on the access link; *ii*) NB-IoT air interface based on Release 14 and 15 [32]–[34] in the user link; *iii*) a standalone NB-IoT deployment with a carrier frequency $f_c = 2$ GHz; *iv*) the UEs are fixed on Earth and no mobility is foreseen for them. Please note that the selected carrier frequency is in line with standard specification for NTN networks [12]. Last but not least, we assume that the targeted area is isolated from the terrestrial coverage, hence no interference will be introduced in our system architecture under consideration.

The channel can be approximately modeled as additive white Gaussian noise channel by neglecting the multipath fading. This is due to the fact that we are considering a remote area to be covered, and having a perfect line of sight (LoS) transmission can be assumed. Therefore, the only component in our satellite link would be the LoS component impaired by a Doppler shift due to the movement of the satellite.

1) DOWNLINK TRANSMISSION

In the downlink, the transmitted baseband analog signal from the eNB to the UEs can be written as:

$$s(t) = \frac{1}{\sqrt{N}} \sum_{n=0}^{N-1} a[n] e^{j2\pi f_s n t} \cdot u_T(t) \tag{1}$$

where $a[n]$ depicts the symbols (data or pilots) carried by the n-th subcarrier, $u_T(t)$ is a rectangular window function, hence $u_T(t) = 1$ for $0 \leq t \leq T$. Please note that $T = T_s + T_{cp}$ where T_s is the symbol period and T_{cp} is the cyclic prefix length. The parameter $f_s = 1/T_s$ represents the subcarrier spacing. Finally, the received analog signal by the k-th UE after downconversion can be expressed as:

$$\begin{aligned} r_{UE}^k(t) &= e^{j2\pi f_{dk}(t)t} \cdot h_k(t) \cdot s(t) + \omega_k(t) \\ &= e^{j2\pi f_{dc}(t)t} \cdot e^{j2\pi \Delta f_{dk}(t)t} \cdot h_k(t) \cdot s(t) + \omega_k(t) \end{aligned} \tag{2}$$

where $\omega_k(t)$ is the additive white Gaussian noise, $f_{dk}(t)$ is the Doppler shift which has a dependency on time based

on the position of the LEO satellite, $h_k(t)$ are the channel coefficients and $s(t)$ is the transmitted analog baseband signal from the base station eNB. Please note that the Doppler shift can be written as $f_{dk}(t) = f_{dc}(t) + \Delta f_{dk}(t)$, where $f_{dc}(t)$ is the common part of Doppler shift experienced by all the UEs in the coverage area and is given by the Doppler curve of one of the users taken as reference, for example the one in the middle. $\Delta f_{dk}(t)$ is the differential part of the k-th UE which has a dependency on the relative position of UEs with respect to the reference user. From equation (1) and (2), and assuming that the frequency offset of the local oscillator is negligible, the received OFDM symbol of the k-th user of a frame transmitted at time $[t', t' + T]$ after sampling at time $t = lT_s/N$, FFT and equalization can be written in the discrete form as:

$$r_{l,k} = e^{j2\pi\epsilon_k l/N} \cdot a_{l,k} + \omega_{l,k} \tag{3}$$

where $l = 0, 1, \ldots, N-1$ is the subcarrier index, N is the number of subcarriers assigned to the k-th UE (12 in the DL) and $a_{l,k}$ is the l-th modulated symbol (QPSK in DL) of the overall OFDM symbol for the k-th UE. It is worth highlighting that $\epsilon_k = f_{dk}/f_s$ is the normalized Doppler shift with respect to subcarrier spacing. This parameter also drives the performance degradation in our scenario. Please note that the Doppler shift will also have a small variation during each OFDM symbol time. However this time is so small that we assume a constant f_{dk} along $[t', t' + T]$.

2) UPLINK TRANSMISSION

In the uplink, the transmitted signal by the k-th UE to the eNB will have the following form:

$$s_k(t) = \frac{1}{\sqrt{N_k}} \sum_{n=0}^{N_k-1} b_k[n] e^{j2\pi f_s n t} \cdot u_T(t) \tag{4}$$

where $b_k[n]$ are the symbols mapped into subcarriers after applying DFT and N_k is the number of subcarriers assigned for transmission for the k-th UE. As already described in the previous section, the number of subcarriers assigned for transmission can be 1 (single-tone), 3, 6 or 12 (multi-tone). Please note that SC-FDMA with single-tone is mathematically identical to OFDM, because the DFT step can be excluded. The received baseband signal at the eNB is given by the superposition of each signal from UEs:

$$\begin{aligned} r_{eNB}(t) &= \sum_{k=1}^{M} e^{j2\pi f_{dk}(t)t} \cdot h_k(t) \cdot s_k(t) + \omega_k(t) \\ &= e^{j2\pi f_{dc}(t)t} \sum_{k=1}^{M} e^{j2\pi \Delta f_{dk}(t)t} h_k(t) s_k(t) + \omega_k(t) \end{aligned} \tag{5}$$

where M is the number of UEs transmitting at a certain time. It is worth highlighting here that M will have a dependency on the transmission mode used by the UEs (single-tone or multi-tone). For example, for a single-tone SC-FDMA transmission with 15 kHz SCS, there can be a maximum 12 UEs simultaneously transmitting. Again, like in the downlink case, assuming that the frequency offset of the local oscillator is negligible, the received SC-FDMA symbol of the uplink frame transmitted at time $[t', t' + T]$ after sampling at time $t = lT_s/N$, FFT and equalization can be written in the discrete form as:

$$r_l = e^{j2\pi\epsilon l/N} \cdot a_l + \sum_{k=0, k\neq l}^{N-1} a_k + \omega_l \tag{6}$$

where the total number of subcarriers N in this case can be 12 or 48 depending on the SCS used. Please note that with respect to the downlink transmission, here we will have the presence of a second term $\sum_{k=0,k\neq l}^{N-1} a_k$ which characterizes the inter-carrier interference (ICI) coming from k-th symbols (BPSK or QPSK) modulated in the other subcarriers of the overall SC-FDMA symbol. In the downlink transmission, this term is zero, since the subcarriers are strictly orthogonal between them and the whole NB-IoT band is shifted in frequency. Whereas in the uplink transmission this does not hold, because of the presence of a differential Doppler between subcarriers. Due to the slotted structure of SC-FDMA, the subcarriers assigned to different users will arrive to the satellite with different Doppler shifts, negating the orthogonality in the final SC-FDMA signal.

IV. PROBLEM STATEMENT

Following the reasoning of the previous section, both Doppler shift and differential Doppler shift would have an impact in the received symbols at the UE or eNB side. In the literature, there exist methods and solutions to deal with the high Doppler shift over a LEO satellite as already emphasized in Section I. Assuming perfect estimation of Doppler shift at the gateway, using the techniques proposed in [25]–[29], a frequency offset will be applied in the transmitted frequency, such that it will appear to have zero Doppler shift when it arrives to the desired UE placed on the coverage area. The same holds for the uplink case, where the frequency offset now will be applied to the received frequency. By doing so, the only contributor now to the performance degradation would be the ICI coming from differential Doppler part. Of course, if each individual UE can also estimate and pre-compensate its differential Doppler (as in the gateway) before transmitting the signal, the problem can be solved. However, this would raise significantly the complexity in the user side, since it would require a continuous estimation of the satellite position. Taking into account the IoT vision of very low cost and low complex devices, alternative solutions should be found. To this aim, it would be of high importance to firstly quantify the differential Doppler.

In our previous paper [31], we came up with a closed-form expression of the differential Doppler under the coverage area (see equation (7) and (8), as shown at the bottom of the next page), where f is the carrier frequency, r_E is the radius of Earth, r is the orbit radius of the satellite, w_s is the angular velocity of the satellite in the ECI (Earth central inertial) frame and D is the diameter of the coverage area.

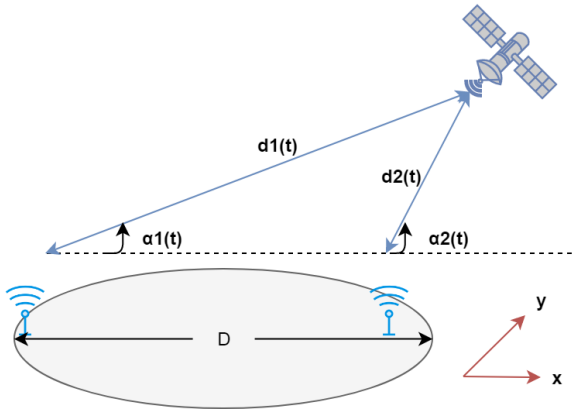

FIGURE 4. Two UE with the maximum differential Doppler shift along x-axis.

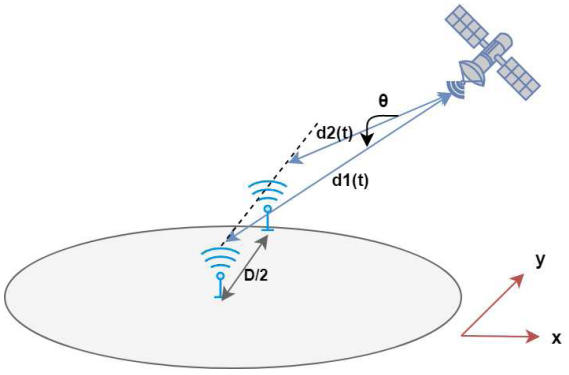

FIGURE 5. Two UE with the maximum differential Doppler shift along y-axis.

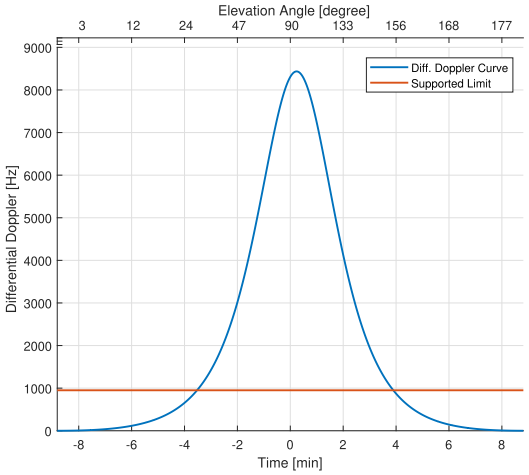

FIGURE 6. Maximum differential Doppler curves along x-axis.

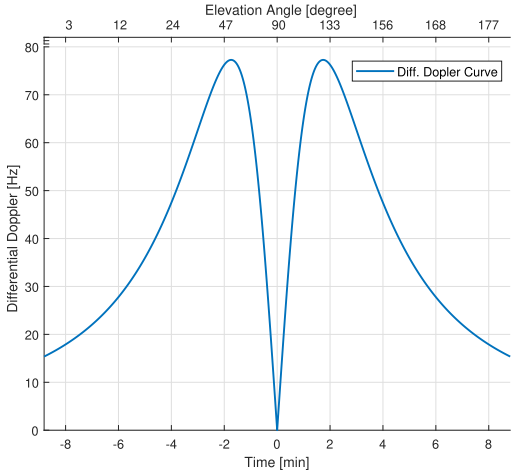

FIGURE 7. Maximum differential Doppler curves along y-axis.

For simplicity, we separated the analysis in two axes, x-axis which has the same direction with the movement of the satellite and y-axis which is the one perpendicular to it (please refer to Figure 4 and 5). It is possible to obtain the differential Doppler curves as a function of elevation angle of the satellite and time, by plugging in the system parameters of our scenario in (7) and (8) and perform numerical simulations. The simulation results are illustrated in Figure 6 and 7. Please note that the region of interest is from 45 to 135 degrees as this is the minimum elevation angle of communication in our scenario. Eventually, it can be observed that the differential Doppler shift achieves the peak values of approximately 8.5 kHz along x-axis and 0.075 kHz along y-axis.

In a terrestrial network, the differential Doppler shift occurs due to the mobility of the users on Earth. In fact, using 3GPP specification about mobile UEs, carrier frequency at 2 GHz, 15 kHz SCS and maximum speed of 500 km/h [36], it can be derived that the standard can support up to 950 Hz of Doppler shift among subcarriers. This means that the standard itself is able to mitigate a loss of orthogonality of up to 950 Hz. Returning the attention to our numerical results, it can be seen that the differential Doppler is much higher than the supported limit along x-axis. Whereas, along y-axis this value is notably lower with respect to the limit, hence we can consider it as negligible. As a consequence, the final received SC-FDMA signal at the eNB will be significantly distorted due to a large amount of overlap between subcarriers

$$\Delta f^{x}_{dmax}(t) = \left| \frac{f w_s r_E}{c} \left(\frac{r\, sin(w_s t) - D}{\sqrt{r_E^2 + r^2 - 2 r_E r\, cos(w_s t) + D^2 - 2Dr\, sin(w_s t)}} - \frac{r\, sin(w_s t)}{\sqrt{r_E^2 + r^2 - 2 r_E r\, cos(w_s t)}} \right) \right| \tag{7}$$

$$\Delta f^{y}_{dmax}(t) = \left| \frac{f w_s r_E r\, sin(w_s t)}{c} \left(\frac{\eta[tg^{-1}(\frac{h}{D/2})]}{\sqrt{r_E^2 + r^2 - 2 r_E r\, cos(w_s t)\eta[tg^{-}1(\frac{h}{D/2})]}} - \frac{1}{\sqrt{r_E^2 + r^2 - 2 r_E r\, cos(w_s t)}} \right) \right| \tag{8}$$

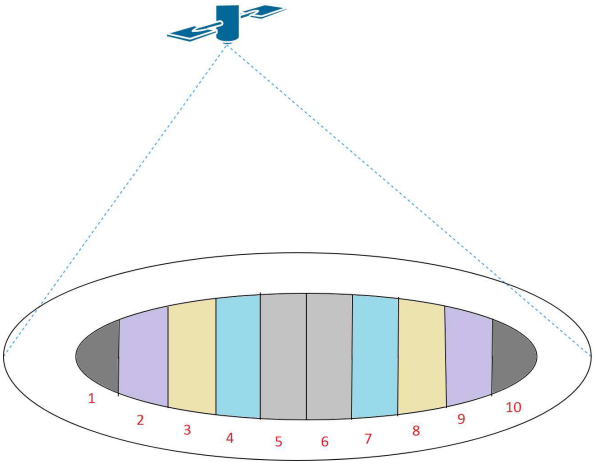

FIGURE 8. Representations of the groups in the coverage region.

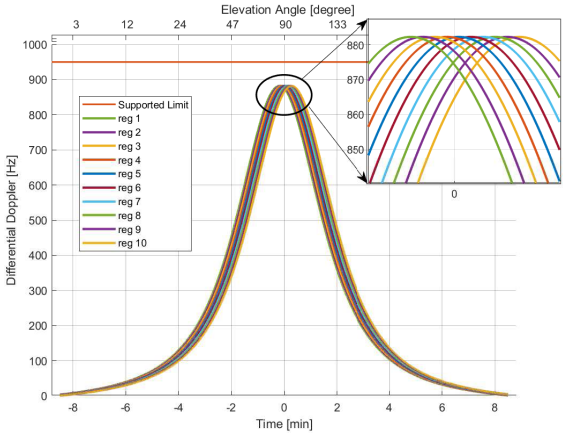

FIGURE 9. Maximum differential Doppler along x-axis in the created groups.

(up to 8.5 kHz), when terminals with large distance in the x-axis are scheduled in the same frame.

V. PROPOSED SOLUTION

In this paper, we come up with a technique to reduce the differential Doppler down to a value supported by the standard, which we calculated to be 950 Hz. Therefore, we propose re-grouping the UEs on the coverage area in such a way that the differential Doppler among users inside each group should be below the allowed threshold. Of course, the number of groups that we need will depend on the value of the differential Doppler at a certain time and elevation angle (see Figure 6). The smaller the differential Doppler, the larger groups we can create. However, considering the worst case scenario, having the peak of differential Doppler, it can be easily calculated that at $D = 20$ km the maximum differential Doppler along x-axis will be below the threshold of 950 Hz. Therefore, for the worst case, 10 groups of UEs will be needed as in Figure 8. It is worth reminding that along the y-axis the differential Doppler is so low that smaller groups are not needed in this direction. By performing numerical simulations, we obtain the maximum differential Doppler curves for all the regions along the x-axis as in Figure 9. It can be noted that now the peak values of differential Doppler in each group is approximately 880 Hz along the x-axis. Finally, the problem to be solved is how to schedule the uplink transmission to the created group of users.

A. GROUP SCHEDULING IN TIME (GS-T)

One way of scheduling the users and assigning appropriate resources is in the time domain. This implies that NB-IoT carrier is assigned for a certain amount of time to each group by the eNB. Thereby, the eNB will be capable of decoding correctly the symbols coming from users situated in the same group no matter how the subcarriers are allocated to the users, as the differential Doppler experienced will be under the desirable limit. Please note that SC-FDMA is still used in the uplink by the UEs inside a group. In addition, it is very important to emphasize that the eNB must know the position of all the UEs, for the purpose of user-grouping and a proper allocation of the resources. As no mobility is assumed for the UEs, it is possible to calibrate their location in the deployment phase of the devices in the coverage area. In the Attach Request Procedure, as described in [37], the UEs will identify themselves in the network by sending their IMSI (International Mobile Subscriber Identity) or old GUTI (Globally Unique Temporary ID) and a map can be created which connects their ID with the location in the region. In all the other procedures and message exchanges, the UE will be identified in the network through this ID, hence its position in the coverage area will be known.

B. GROUP SCHEDULING IN FREQUENCY (GS-F)

Another possibility of assigning the uplink resources to the users is in the frequency domain. In other words, several NB-IoT carriers are needed, and not just one, for the uplink transmission, as in Figure 10. Using secondary carriers in the NB-IoT uplink transmission is totally supported by the standard and specified in the Release 14 [38]. In such a case, we must assign adjacent NB-IoT carriers to adjacent groups, because the differential Doppler between adjacent groups is the smallest possible. It can be calculated that for the worst case scenario (maximum differential Doppler), we will need to create 20 groups. By doing so, we maintain the overlap under the requested limit, not only inside each NB-IoT carrier but also among adjacent carriers. The reason we need to double the number of regions, with respect to the GS-T case, is that now the maximum distance of two UE part of adjacent groups will be 40 km. Finally, we will need an uplink bandwidth of $B = 20 * 180 \ \ kHz = 3,6 \ MHz$ for GS-F.

It is worth highlighting here that the above techniques have been already proposed in the previous work [31], but with different names. We decided to change the names in this paper, since the previous ones were confusing and misleading for the reader.

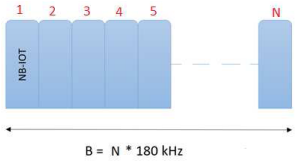

FIGURE 10. Needed resources in the uplink transmission.

To conclude, the advantage of this scheduling approach is that the UEs placed in the coverage region will follow the same procedures and use the same technical specifications as in the terrestrial network, since the uplink scheduling and time-frequency resource assignment is done at the eNB (refer to Section II). In fact, it is the eNB which needs to continuously track and estimate the differential Doppler shift, and re-group the users accordingly. Based on the above considerations, the eNB schedules the users in the uplink through the information sent in the NPDCCH, in order to assure that at any time the resulting SC-FDMA waveform coming at the eNB, falls into the standard specification. The strong assumption behind this solution is the non-mobility of the NB-IoT devices, which for many monitoring IoT applications is reasonable.

VI. PERFORMANCE EVALUATION

The aim of this section is to validate the proposed scheduling techniques for our system architecture under consideration. To this aim, we implement in Matlab the PHY layer of an end-to-end NB-IoT over LEO satellite system, incorporating the technical specifications of NB-IoT standard [32]–[34] with the scheduling techniques, and evaluate the NPUSCH channel performance in terms of block error rate (BLER) versus signal to noise ratio (SNR). We use as a starting framework the already available NB-IoT Matlab toolbox [39] to simulate the NPUSCH uplink transmission. Since the toolbox is designed for a terrestrial NB-IoT network and a point to point communication, needed modifications are implemented in order to adapt it with our scenario. The obtained results are then compared with the case of a perfect synchronous communication link and with the case where the GS approach is not used.

A. SIMULATOR DESIGN

The block diagram of our simulator is shown in Figure 11 and the main parameters are listed in Table 4. We consider a certain number of NB-IoT devices uniformly distributed in the coverage area that have data to transmit in the uplink through NPUSCH. The coding and SC-FDMA modulation follow the steps as described in the standard. We fix a single-tone transmission mode for all the users, since it corresponds to the worst case scenario (highest ICI). In addition, we fix the TBS size to be the same for all the users (not realistic) to facilitate the scheduling part of the different NPUSCH channels. This does not impact our simulator because the focus is to show the performance gain of GS-T and GS-F.

TABLE 4. Parameters for NPUSCH Simulation.

Parameter	Value
N FFT	128
Bandwidth GS-T	180 kHz
Bandwidth GS-F	180(n+1) kHz
SCS	15 kHz
Modulation Format	single-tone SC-FDMA
Modulation Order	QPSK
Sub-carrier Mapping	Random with GS-T (GS-F)
Coding Scheme	1/3 Turbo Code
CRC Bits	24
NPUSCH Repetition	1
NRU	1
TBS size	72 bits
Channel	AWGN
HARQ	N/A

Overall, the following steps are performed for the BLER calculation:

- The resource grids populated with NPUSCH from different UE is generated. Each NPUSCH will occupy 1 subcarrier in the frequency domain and 16 uplink slots (8 ms TTI) in the time domain (refer to Table 1). This is the corresponding RE for single-tone operation. It can be noted that for GS-T, 12 users can be scheduled simultaneously, whereas for GS-F, $12(n+1)$ users can be scheduled, where n is the number of secondary NB-IoT carriers. Each NPUSCH will contain the useful transmitted bits (TBS), generated randomly, and other redundancy bits added by the coder part. Since the time-frequency resources for each NPUSCH are fixed, as mentioned above, changing the TBS will change the coding rate. However, throughout this simulation, we keep the $TBS = 72$ bits fixed. Last but, not least, we make sure that each UE occupies different subcarriers in the frequency domain and the choice of the subcarrier is random.
- The baseband waveform for each UE is then created through SC-FDMA modulation.
- A random Doppler shift is then applied to each waveform taking random values from $[-440\ +440]$ Hz for GS-T/GS-F and from $[-4250\ +4250]$ for the case of no GS. This allows to create the differential Doppler shift among carriers from [0 880] Hz for GS-T/GS-F and from [0 8500] Hz without GS (refer to Figure 6 and 9).
- The individual baseband waveforms are then summed up, though forming the final SC-FDMA waveform which now will be distorted due to the overlap among subcarriers and pass it through the AWGN channel.
- The receiver operations are performed and the corresponding NPUSCH coming from different UEs are decoded.
- The performance of the NPUSCH is finally determined by counting the number of erroneous TBS. We run the simulations in order to assure at least 100 erroneous blocks for each SNR value.

Finally, we compare the obtained results with the case of a perfectly synchronous waveform. In fact, for such case,

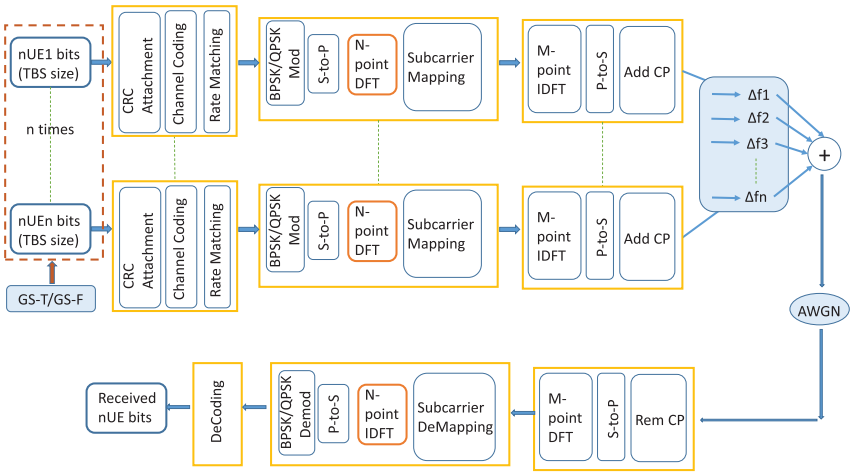

FIGURE 11. Block diagram of the baseband simulator.

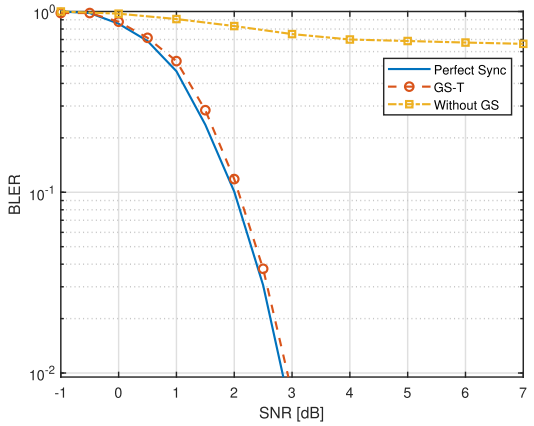

FIGURE 12. Simulation results for GS-T.

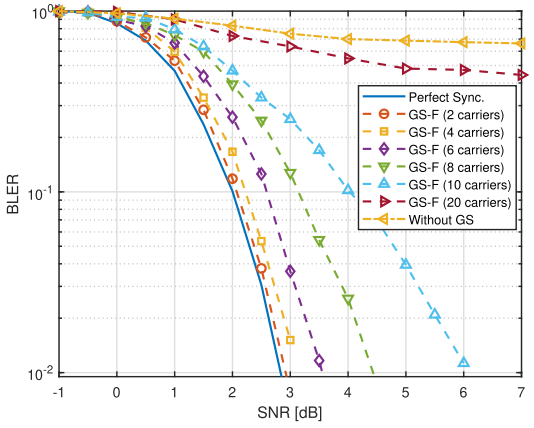

FIGURE 13. Simulation results for GS-F.

we just neglect the part where we apply the Doppler shifts among subcarriers which contain the NPUSCH channels, resulting in a perfectly orthogonal SC-FDMA waveform.

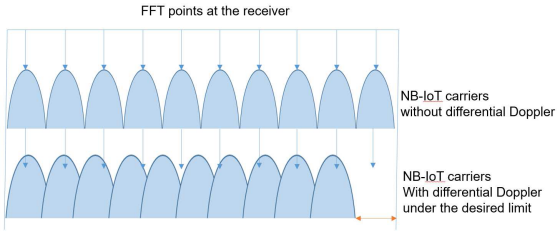

FIGURE 14. Bandwidth compression effect in GS-F.

B. SIMULATION RESULTS AND DISCUSSIONS

From the plotted results shown in Figure 12 and 13, it can be noted that the performance of the NPUSCH when we use GS-T is very close to the one where the waveform is perfectly synchronized. Without GS-T, the results demonstrate that we cannot have a reliable communication under the simulated SNR and the degradation of performance with respect to the perfectly synchronized waveform is huge.

On the other hand, using GS-F the performance is dependent on the secondary NB-IoT carriers that we use. The more secondary carriers we have, the more performance degradation the uplink transmission will experience. This is due to the band compression effect that will happen in our scenario (Figure 14). Even though by adding secondary carriers, we make sure that the differential Doppler remains under the supported limit, it will sum up and cause a shrink of the bandwidth, which the eNB is not aware of and cannot compensate the ICI coming from it. As a matter of fact, without modifying the receiver the eNB fails to decode and demodulate correctly the data when the number of secondary carriers is high. However, it is worth noting that by keeping the number of secondary carriers low, this effect will be relaxed and we can guarantee a reliable communication having a lower performance degradation with respect to the ideal case.

TABLE 5. Code Rates for all the TBS.

I_{TBS}	I_{RU}							
	0	1	2	3	4	5	6	7
0	0.14 (0.21)	0.10 (0.15)	0.09 (0.14)	0.10 (0.15)	0.10 (0.15)	0.10 (0.15)	0.10 (0.15)	0.10 (0.15)
1	0.17 (0.26)	0.14 (0.21)	0.13 (0.20)	0.15 (0.23)	0.14 (0.21)	0.13 (0.20)	0.12 (0.18)	0.13 (0.20)
2	0.19 (0.29)	0.17 (0.26)	0.19 (0.29)	0.17 (0.26)	0.16 (0.24)	0.16 (0.24)	0.15 (0.23)	0.16 (0.24)
3	0.22 (0.33)	0.22 (0.33)	0.23 (0.35)	0.20 (0.30)	0.19 (0.29)	0.20 (0.30)	0.20 (0.30)	0.21 (0.32)
4	0.28 (0.42)	0.25 (0.38)	0.27 (0.41)	0.24 (0.36)	0.24 (0.36)	0.25 (0.38)	0.25 (0.38)	0.25 (0.38)
5	0.33 (0.50)	0.29 (0.44)	0.29 (0.44)	0.31 (0.47)	0.31 (0.47)	0.31 (0.47)	0.31 (0.47)	0.31 (0.47)
6	0.39 (0.59)	0.35 (0.53)	0.32 (0.48)	0.36 (0.54)	0.37 (0.56)	0.36 (0.54)	0.36 (0.54)	0.36 (0.54)
7	0.44 (0.66)	0.43 (0.65)	0.41 (0.62)	0.43 (0.65)	0.42 (0.63)	0.43 (0.65)	0.44 (0.66)	
8	0.5 (0.75)	0.49 (0.74)	0.48 (0.72)	0.49 (0.74)	0.49 (0.74)	0.48 (0.72)		
9	0.56 (0.84)	0.56 (0.84)	0.56 (0.84)	0.56 (0.84)	0.56 (0.84)	0.56 (0.84)		
10	0.58 (0.87)	0.61 (0.92)	0.61 (0.92)	0.61 (0.92)	0.62 (0.93)	0.59 (0.89)		
11	0.69	0.69	0.70	0.69	0.71			
12	0.81	0.81	0.81	0.89				

*The values in brackets correspond to the code rates in case of single-tone transmission.

VII. NPUSCH THROUGHPUT ANALYSIS

The aim of this section is to demonstrate the achievable throughput of our system architecture, in order to stress out the limitations coming from the satellite channel. The achievable throughput of the NPUSCH is directly dependent on the MCS and the transmission mode used (single/multi-tone). For example, it is well known that the peak NPUSCH data rate in the terrestrial NB-IoT standard is achieved at MCS level 12 ($TBS = 1000$ bits and $N_{RU} = 4$), and it can easily calculated to be 250 kbps [40]. However, each MCS level will require a certain SNR in order to guarantee a specific BLER target. In this context, to make the throughput analysis we need the following: a) to analyze the SNR demand for each MCS level selection, and b) the link budget analysis of our satellite-based NB-IoT architecture in order to obtain the SNR as a function of satellite elevation angle. As a result, we repeat the simulations in the previous sections, but now using all the TBS available in Table 2. Please note that in the remainder of the paper, we will use only the GS-T method, since it outperforms the GS-F, as already shown.

A. BLER VERSUS SNR USING GS-T WITH DIFFERENT MCS

Starting from Table 2 and considering the coder design of NB-IoT, it is possible to derive the NPUSCH code rates using the following formula as in [41]:

$$C = \frac{TBS + 24}{T_{sc} \cdot n_b} \tag{9}$$

where 24 are the number of Cyclic Redundancy Checksum (CRC) bits, T_{sc} is the total number subcarriers available for transmitting the transport block and n_b is the number of bits per subcarrier. Please note that T_{sc} depends on the number of tones used for transmission, whereas n_b depends on the modulation order. The achieved code rate results shown in Table 5 match also with the derivations in [42]. Figure 15 and 17 demonstrate the simulation results for single-tone transmission and multi-tone transmissions respectively for different MCS levels. We obtain the BLER-SNR curves by repeating the simulations as in the previous section only for GS-T, using the block diagram in Figure 11,

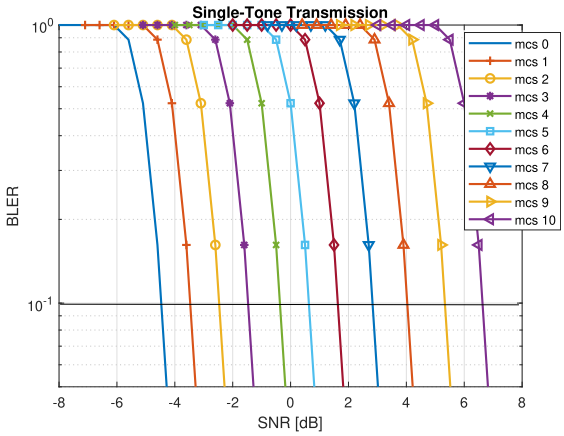

FIGURE 15. Simulation results for GS-T with different MCS levels.

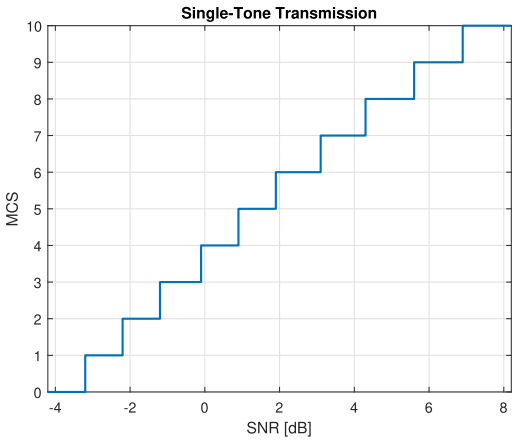

FIGURE 16. Step function for target *BLER* $= 10^{-1}$.

but now changing the MCS level (TBS and N_{RU}). Please note that for each MCS level, there are more than one TBS possible to use (corresponding to different N_{RU}). However, their performance is similar since the coding rates inside the same MCS level is approximately the same. For simplicity, we have shown in the figure only the BLER-SNR curve with the best performance for each MCS level. Fixing the BLER

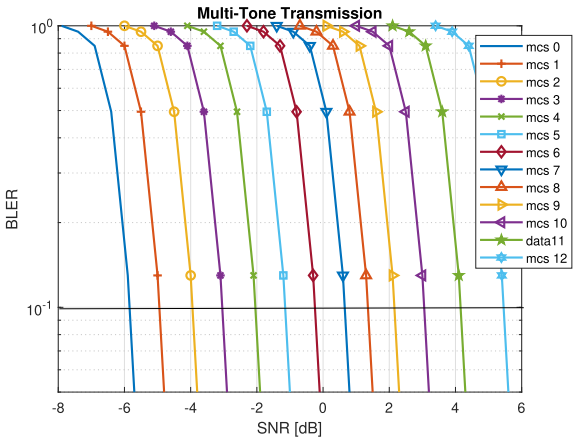

FIGURE 17. Simulation results for GS-T with different MCS levels.

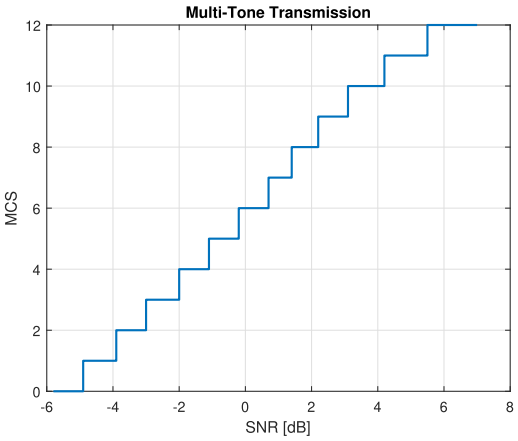

FIGURE 18. Step function for target $BLER = 10^{-1}$.

target to $BLER = 10^{-1}$, as specified in the standard for NPUSCH [43], it is possible to build the step function (please refer to Figure 16 and 18), which shows the required SNR for each MCS level. Having obtained the above results, it is highly important now to assess the link budget that we have in our satellite-based NB-IoT scenario.

B. LINK BUDGET OF OUR NB-IOT-SAT ARCHITECTURE

To evaluate the link budget of our scenario, we use the System Tool Kit (STK) [44]. Through this software, it is possible to implement our NB-IoT over LEO satellite scenario under the predefined and assumed parameters as described in Section II. What we need to add are the parameters of the transmitting antenna (UE) and receiving antenna (satellite). As a matter of fact, for the UEs antenna in the coverage regions, we use the standard specification [45]. These NB-IoT devices fall into the Cat-NB2 category, having an isotropic antenna with 23 dBm of maximum transmitted power and 0 dBi antenna gain. For the satellite antenna characteristic, we use some existing models in the STK tool. Hence, we use a Gaussian model for the antenna pattern operating at carrier frequency $f_c = 2$ GHz with a diameter $d = 0.3$ m and efficiency 55%. It can be derived that the main lobe gain of this antenna would be approximately 13 dB and the beamwidth 39 degrees. Finally, we assume a constant system noise temperature of 290 K.

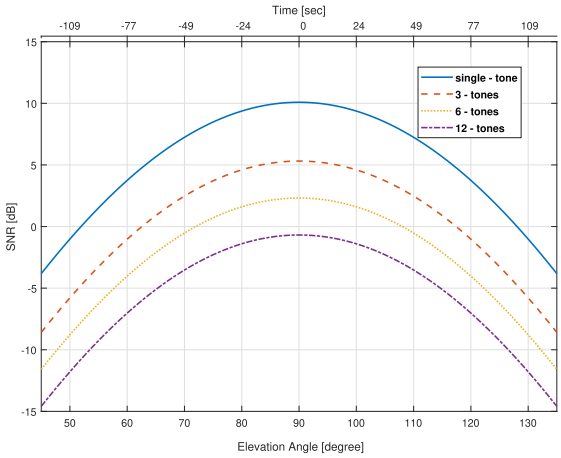

FIGURE 19. Link budget as a function of satellite elevation angle and time.

It is possible to obtain the results demonstrated in Figure 19 of the received SNR at the eNB as a function of elevation angle and time for different transmission modes. Please note that the obtained curves are only for the center of the coverage area. The same holds for any position in this area, with only a small shift in time. Since the UE antenna specifications are fixed by the standard, changing the satellite antenna model and parameters would result in different SNR curves. It can be noted that depending on the number of tones we use for transmission (1, 3, 6, 12), the SNR at the receiver will change. This is quite straightforward and is due to the fact that the power of the NB-IoT devices is fixed. Using fewer tones for transmission means modulating the data in a smaller bandwidth. As a consequence, this would result in a higher SNR at the receiver side. At this point, by combining the results obtained here, with those of the previous subsection, it is possible to derive the achievable NPUSCH data rates as a function of elevation angle and time.

C. ACHIEVABLE NPUSCH DATA RATE FOR EACH USER AND FOR THE ENTIRE CELL

As we mentioned before, different MCS would result in different achievable NPUSCH data rates. For this calculation, we can use the following formula: $Throughput = TBS/TTI$, where TTI will depend on the number of tones used and the number of resource units N_{RU} for scheduling the NPUSCH. For each MCS level, we choose the (I_{TBS}, N_{RU}) couple which gives us the maximum data rate in that particular level. The results in Figure 20 show the achievable data rates as a function of the satellite elevation angle and time, derived from the MCS level selection under a specific SNR, by simply combining the results shown in Figure 16,18 and 19. It can be noted that for single-tone transmission we have enough

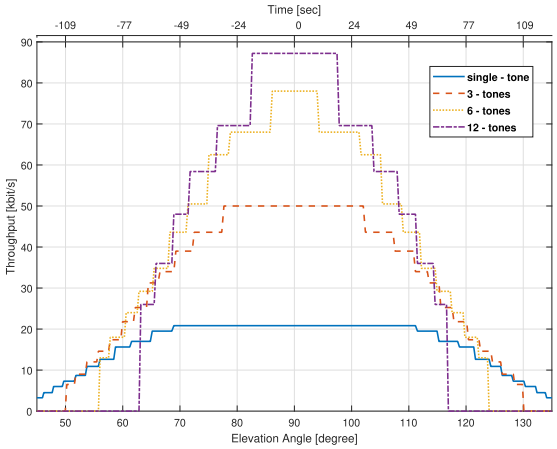

FIGURE 20. User NPUSCH achievable data rate without repetitions.

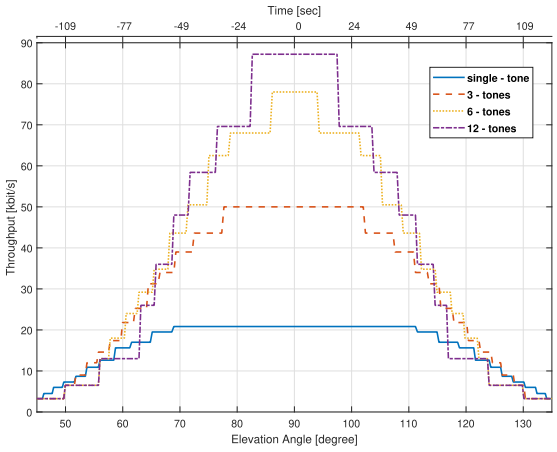

FIGURE 21. User NPUSCH achievable data rate with repetitions.

SNR to close the link regardless of the elevation angle and use all the possible MCS. However, the lower the elevation angle, the lower the data rate, since we are constrained to use a lower MCS in such a case. On the other hand, in the case of multi-tone transmission, the link budget can be closed only for higher elevations angles and not all the MCS are reachable. Of course, this would have an impact in the time-duration the transmission is possible and in the maximum achievable data rates.By enabling repetition of the NPUSCH channel, as defined in the standard, the coverage can be enhanced, hence assuring a reliable communication even at lower SNR. However, the drawback of allowing NPUSCH repetition, is that we loose in terms of data rate since to send the same amount of bits, we will need more resources in time. The results when we enable repetition code as well, are illustrated in Figure 21. Last but not least, it is worth deriving here the achievable cell data rate. Depending on the number of tones, the number of users that can transmit simultaneously will change. Basically, in 12-tone operation mode, only one UE can transmit data in the uplink, hence the achievable cell data rate corresponds to the user one. Whereas, for 1,3,6 tone of operation, the data rate will be 12,4,2 times

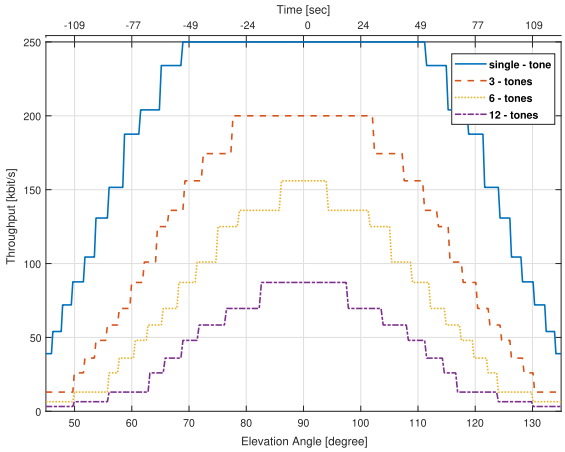

FIGURE 22. Cell NPUSCH achievable data.

higher respectively, as demonstrated in Figure 22. It is worth noting that in our scenario, using single-tone transmission would be favourable because it demonstrates to be more spectrally efficient.

VIII. CONCLUSIONS

In this paper, we considered an NB-IoT over LEO satellite architecture, in order to extend the coverage of terrestrial NB-IoT in remote areas and satisfy its goal of ubiquitous global coverage. The problem of the differential Doppler shift is formulated, by assuming a perfect estimation and compensation at the gateway of the residual Doppler part, which is experienced by all the NB-IoT devices in the coverage area. In order to solve the differential Doppler problem, an uplink scheduling technique is proposed, able to mitigate the differential Doppler down to a value tolerable by the standard. In particular, by implementing GS-T and GS-F, we reduce the differential Doppler from 8.5 kHz down to 880 Hz. The performance of the proposed schemes is assessed through numerical simulations of the NPUSCH channel and compared with the case where the differential Doppler shift is not mitigated. The simulation results validate the proposed scheduling technique and demonstrate that the GS-T outperforms GS-F, since the later has a dependency on the number of secondary NB-IoT carriers used for transmission. In addition, the throughput analysis of the NPUSCH channel is shown, in order to highlight the boundaries and limitations coming from the presence of a satellite channel in such systems. In fact, in our scenario we demonstrate that using single tone-transmission mode is favourable because it results to be more spectrally efficient with respect to the multi-tone case. A multi-tone transmission is unable to reach the highest MCS levels, where the throughput is higher, since the required SNR for those MCS levels cannot be satisfied.

The advantage of the proposed scheduling technique relative to the recent literature in the field, is that it does not increase the complexity at the user side. Consequently, no modifications are needed for the NB-IoT devices, assuring

a seamless connectivity and service regardless of the presence of a satellite or a terrestrial network, which aligns with the aim of having an integrated satellite-terrestrial network. Last but not least, even though we formulate the problem and validate the techniques using a satellite based NB-IoT system, the proposed techniques are applicable to other 5G mMTC applications, such as LTE-M, with only small adaptations. The reason behind that is due to the similarity in the PHY layer of all the 5G mMTC standards.

In the future work, we will evaluate the proposed scheduling technique under realistic IoT traffic. The aim will be to study the ability of the proposed technique to satisfy different traffic demands coming from IoT devices, in the case of a single LEO satellite and a constellation of LEO satellites. In addition, we will take into account the case where the users can move in the coverage area and alternative solutions should be found in order to make the proposed scheduling technique still feasible.

REFERENCES

[1] A. Al-Fuqaha, M. Guizani, M. Mohammadi, M. Aledhari, and M. Ayyash, "Internet of Things: A survey on enabling technologies, protocols, and applications," *IEEE Commun. Surveys Tuts.*, vol. 17, no. 4, pp. 2347–2376, 4th Quart., 2015.
[2] M. R. Palattella *et al.*, "Internet of Things in the 5G era: Enablers, architecture, and business models," *IEEE J. Sel. Areas Commun.*, vol. 34, no. 3, pp. 510–527, Mar. 2016.
[3] L. Da Xu, W. He, and S. Li, "Internet of Things in industries: A survey," *IEEE Trans. Ind. Informat.*, vol. 10, no. 4, pp. 2233–2243, Nov. 2014.
[4] G. A. Akpakwu, B. J. Silva, G. P. Hancke, and A. M. Abu-Mahfouz, "A survey on 5G networks for the Internet of Things: Communication technologies and challenges," *IEEE Access*, vol. 6, pp. 3619–3647, 2018.
[5] E. Borgia, "The Internet of Things vision: Key features, applications and open issues," *Comput. Commun.*, vol. 54, pp. 1–31, Dec. 2014. [Online]. Available: http://www.sciencedirect.com/science/article/pii/S0140366414003168
[6] *IMT Vision–Framework and Overall Objectives of the Future Development of IMT for 2020 and Beyond*, Int. Telecommun. Union, Geneva, Switzerland, 2015. [Online]. Available: https://www.itu.int/dms_pubrec/itu-r/rec/m/R-REC-M.2083-0-201509-I!!PDF-E.pdf
[7] *LTE; Evolved Universal Terrestrial Radio Access (E-UTRA); Radio Resource Control (RRC); Protocol Specification; (Release 13), Version 13.2.0*, document 3GPP 36.331, Aug. 2016.
[8] *Interim Conclusions for IoT in REL-16*, document 3GPP, TSG RAN Meeting 79 RP-180581, Chennai, India, Mar. 2016.
[9] *3rd Generation Partnership Project; Technical Specification Group Services and System Aspects; Study on Cellular Internet of Things (IoT) Support and Evolution for the 5G System (Release 16), Version 16.0.0*, document 3GPP 23.724, Dec. 2018.
[10] L. Vangelista, A. Zanella, and M. Zorzi, "Long-range IoT technologies: The dawn of LoRa," in *Future Access Enablers for Ubiquitous and Intelligent Infrastructures*, V. Atanasovski and A. Leon-Garcia, Eds. Cham, Switzerland: Springer, 2015, pp. 51–58.
[11] SigFox, "Technical overview," SigFox, Toulouse, France, White Paper, May 2017. [Online]. Available: https://www.disk91.com/wp-content/uploads/2017/05/4967675830228422064.pdf
[12] *Technical Specification Group Radio Access Network; Study on New Radio (NR) to Support non Terrestrial Networks; (Release 15), Version 15.0.0*, document 3GPP TR 38.811, Jun. 2018.
[13] S. Cioni, R. De Gaudenzi, O. Del Rio Herrero, and N. Girault, "On the satellite role in the era of 5G massive machine type communications," *IEEE Netw.*, vol. 32, no. 5, pp. 54–61, Sep./Oct. 2018.
[14] N. Alagha, "Satellite air interface evolutions in the 5G and IoT era," *ACM SIGMETRICS Perform. Eval. Rev.*, vol. 46, no. 3, pp. 93–95, Jan. 2019. doi: 10.1145/3308897.3308941.
[15] S. Scalise, C. P. Niebla, R. De Gaudenzi, O. del Rio Herrero, D. Finocchiaro, and A. Arcidiacono, "S-MIM: A novel radio interface for efficient messaging services over satellite," *IEEE Commun. Mag.*, vol. 51, no. 3, pp. 119–125, Mar. 2013.
[16] R. De Gaudenzi, O. Del Rio Herrero, G. Gallinaro, S. Cioni, and P.-D. Arapoglou, "Random access schemes for satellite networks, from VSAT to M2M: A survey," *Int. J. Satell. Commun. Netw.*, vol. 36, no. 1, pp. 66–107, 2018. doi: 10.1002/sat.1204.
[17] N. Celandroni, E. Ferro, A. Gotta, G. Oligeri, C. Roseti, M. Luglio, I. Bisio, M. Cello, F. Davoli, A. D. Panagopoulos, M. Poulakis, S. Vassaki, T. De Cola, M. A. Marchitti, Y. F. Hu, P. Pillai, S. Verma, K. Xu, and G. Acar, "A survey of architectures and scenarios in satellite-based wireless sensor networks: System design aspects," *Int. J. Satell. Commun. Netw.*, vol. 31, no. 1, pp. 1–38, 2012. doi: 10.1002/sat.1019.
[18] M. Gineste, T. Deleu, M. Cohen, N. Chuberre, V. Saravanan, V. Frascolla, M. Mueck, E. C. Strinati, and E. Dutkiewicz, "Narrowband IoT service provision to 5G user equipment via a satellite component," in *Proc. IEEE Globecom Workshops (GC Wkshps)*, Dec. 2017, pp. 1–4.
[19] Z. Qu, G. Zhang, H. Cao, and J. Xie, "LEO satellite constellation for Internet of Things," *IEEE Access*, vol. 5, pp. 18391–18401, 2017.
[20] M. de Sanctis, E. Cianca, G. Araniti, I. Bisio, and R. Prasad, "Satellite communications supporting Internet of remote things," *IEEE Internet Things J.*, vol. 3, no. 1, pp. 113–123, Feb. 2016.
[21] 3GPP, *NR-NTN: Link Budget Analysis*, document 3GPP R1-1805078, TSG RAN WG1 Meeting 92bis, Sanya, China, Apr. 2018.
[22] *Frequency Compensation in NTN*, document 3GPP RP-1813362, TSG RAN WG1 Meeting 95, Spokane, USA, Nov. 2018.
[23] A. Guidotti, A. Vanelli-Coralli, M. Conti, S. Andrenacci, S. Chatzinotas, N. Maturo, B. Evans, A. Awoseyila, A. Ugolini, T. Foggi, L. Gaudio, N. Alagha, and S. Cioni, "Architectures and key technical challenges for 5G systems incorporating satellites," *IEEE Trans. Veh. Technol.*, vol. 68, no. 3, pp. 2624–2639, Mar. 2019.
[24] M.-H. You, S.-P. Lee, and Y. Han, "Adaptive compensation method using the prediction algorithm for the Doppler frequency shift in the LEO mobile satellite communication system," *ETRI J.*, vol. 22, no. 4, pp. 32–39, Dec. 2000.
[25] A. Guidotti, A. Vanelli-Coralli, T. Foggi, G. Colavolpe, M. Caus, J. Bas, S. Cioni, and A. Modenini, "LTE-based satellite communications in LEO mega-constellations," *Int. J. Satell. Commun. Netw.*, to be published. doi: 10.1002/sat.1258.
[26] O. Kodheli, A. Guidotti, and A. Vanelli-Coralli, "Integration of satellites in 5G through LEO constellations," in *Proc. IEEE Global Commun. Conf. GLOBECOM*, Dec. 2017, pp. 1–6.
[27] J. Lin, Z. Hou, Y. Zhou, L. Tian, and J. Shi, "Map estimation based on Doppler characterization in broadband and mobile LEO satellite communications," in *Proc. IEEE 83rd Veh. Technol. Conf. (VTC Spring)*, May 2016, pp. 1–5.
[28] J.-J. van de Beek, M. Sandell, and P. O. Borjesson, "ML estimation of time and frequency offset in OFDM systems," *IEEE Trans. Signal Process.*, vol. 45, no. 7, pp. 1800–1805, Jul. 1997.
[29] H. Bolcskei, "Blind estimation of symbol timing and carrier frequency offset in wireless OFDM systems," *IEEE Trans. Commun.*, vol. 49, no. 6, pp. 988–999, Jun. 2001.
[30] V. Nair, "Evaluating the suitability of narrowband Internet-of-Things (NB-IoT) for smart grids," M.S. thesis, TU Delft Elect. Eng., Math. Comput. Sci., Delft, The Netherlands, 2017.
[31] O. Kodheli, S. Andrenacci, N. Maturo, S. Chatzinotas, and F. Zimmer, "Resource allocation approach for differential Doppler reduction in NB-IoT over LEO satellite," in *Proc. 9th Adv. Satell. Multimedia Syst. Conf.*, Sep. 2018, pp. 1–8.
[32] *LTE; Evolved Universal Terrestrial Radio Access (E-UTRA); Physical Channels and Modulation; Version 15.3.0; (Release 15)*, document 3GPP TS 36.211, Oct. 2018.
[33] *LTE; Evolved Universal Terrestrial Radio Access (E-UTRA); Multiplexing and channel coding; Version 15.3.0; (Release 15)*, document 3GPP TS 36.212, Oct. 2018.
[34] *LTE; Evolved Universal Terrestrial Radio Access (E-UTRA); Physical Layer Procedures; (Release 14)*, 3GPP TS 36.213, Oct. 2018.
[35] N. Mangalvedhe, R. Ratasuk, and A. Ghosh, "NB-IoT deployment study for low power wide area cellular IoT," in *Proc. IEEE 27th Annu. Int. Symp. Pers., Indoor, Mobile Radio Commun. (PIMRC)*, Sep. 2016, pp. 1–6.
[36] *Requirements for Evolved UTRA (E-UTRA) and Evolved UTRAN (E-UTRAN) (Release 9)*, document 3GPP TR 25.913, Feb. 2010.
[37] *Technical Specification Group Core Network and Terminals; Non-Access-Stratum (NAS) protocol for Evolved Packet System (EPS); Stage 3 (Release 13)*, document 3GPP TS 24.301, Sep. 2016.
[38] A. Hoglund, X. Lin, O. Liberg, A. Behravan, E. A. Yavuz, M. Van Der Zee, Y. Sui, T. Tirronen, A. Ratilainen, and D. Eriksson, "Overview of 3GPP release 14 enhanced NB-IoT," *IEEE Netw.*, vol. 31, no. 6, pp. 16–22, Nov./Dec. 2017.

[39] MATLAB NB-IoT Modelling Toolbox. *NB-IoT NPUSCH Block Error Rate Simulation*. Accessed: Nov. 5, 2018. [Online]. Available: https://nl.mathworks.com/help/lte/examples/nb-iot-npusch-block-error-rate-simulation.html
[40] R. Ratasuk, N. Mangalvedhe, J. Kaikkonen, and M. Robert, "Data channel design and performance for LTE narrowband IoT," in *Proc. IEEE 84th Veh. Technol. Conf. (VTC-Fall)*, Sep. 2016, pp. 1–5.
[41] H. Chung, S. Lee, and J. Jeong, "NB-IoT optimization on paging MCS and coverage level," in *Proc. 15th Int. Symp. Wireless Commun. Syst. (ISWCS)*, Aug. 2018, pp. 1–5.
[42] O. Liberg, E. Wang, J. Bergman, J. Sachs, and M. Sundberg, *Cellular Internet of Things: Technologies, Standards, and Performance*. Amsterdam, The Netherlands: Elsevier, 2017.
[43] *3rd Generation Partnership Project; Technical Specification Group Radio Access Network; Evolved Universal Terrestrial Radio Access (E-UTRA); LTE Coverage Enhancements (Release 11)*, document 3GPP TR 36.824, Jun. 2012.
[44] Systems Tool Kit. *STK*. Accessed: Sep. 14, 2018. [Online]. Available: https://www.agi.com/products/engineering-tools
[45] *LTE; Evolved Universal Terrestrial Radio Access (E-UTRA); User Equipment (UE) Radio Transmission and Reception (Release 14)*, document 3GPP TS 36.101, Apr. 2017.

OLTJON KODHELI received the master's degree *(cum laude)* in electronic engineering from the University of Bologna, Italy, in 2016.

From 2017 to 2018, he was with the Department of Electrical and Information Engineering (DEI), University of Bologna, for performing research related to 5G Radio Access Network. Since 2018, he has been a Doctoral Researcher with the Interdisciplinary Centre for Security, Reliability and Trust, University of Luxembourg. His research interests include PHY layer design for wireless communication systems, satellite communications, and their integration with terrestrial networks. He holds a grant for his Ph.D. project received from Luxembourg National Research Fund (FNR), under Industrial Fellowship Scheme, with industrial partner SES S.A.

STEFANO ANDRENACCI received the M.S. degree *(cum laude)* in telecommunication engineering from the Polytechnic University of Marche, Ancona, Italy, in 2008, and the Ph.D. degree in telecommunication engineering from the Department of Biomedical Engineering, Electronics and Telecommunications, Polytechnic University of Marche, in 2011. During his Ph.D., he collaborated with Aethra spa, Ancona, on immersive telepresence systems and with Mavigex srl, Bologna, on the implementation of digital satellites receivers.

He is currently an Engineer for satellite communication systems at SES S.A. From 2011 to 2014, he was a Postdoctoral Researcher with the Interdepartmental Centre for Industrial Research on Information and Communication Technologies, University of Bologna, where he worked on interference management techniques under some ESA research projects and on hardware implementation of satellite terminals under some ESA technological development projects. From 2014 to 2015, he was a Postdoctoral Researcher with the Department of Electrical and Information Engineering "Guglielmo Marconiâ", University of Bologna. From 2015 to 2018, he was a Research Associate with the Interdisciplinary Centre for Security, Reliability and Trust, University of Luxembourg. His research interests include interference management techniques, synchronization chain design and synchronization techniques for digital receivers, DVB-S2/S2x systems, DVB-RCS2 systems, software-defined radios (SDR), and spread spectrum systems.

NICOLA MATURO received the M.S. degree *(cum laude)*in electronic engineering and the Ph.D. degree in telecommunication engineering from the Polytechnic University of Marche, Ancona, Italy, in 2012 and 2015, respectively.

From 2016 to 2017, he was a Postdoctoral Researcher with the Department of Information Engineering, Polytechnic University of Marche. From 2015 to 2016, he was a Consultant for Deimos Engenharia, Lisbon. Since 2017, he has been a Research Associate with the Interdisciplinary Centre for Security, Reliability and Trust, University of Luxembourg. His research interests include error correcting codes and decoding algorithms for space communications.

SYMEON CHATZINOTAS received the M.Eng. degree in telecommunications from the Aristotle University of Thessaloniki, Thessaloniki, Greece, in 2003, and the M.Sc. and Ph.D. degrees in electronic engineering from the University of Surrey, Surrey, U.K., in 2006 and 2009, respectively.

He is currently the Deputy Head of the SIGCOM Research Group, Interdisciplinary Centre for Security, Reliability, and Trust, University of Luxembourg, Luxembourg, and also a Visiting Professor with the University of Parma, Italy. He was involved in numerous research and development projects for the Institute of Informatics Telecommunications, National Center for Scientific Research Demokritos, the Institute of Telematics and Informatics, Center of Research and Technology Hellas, and the Mobile Communications Research Group, Center of Communication Systems Research, University of Surrey. He has more than 300 publications, 3000 citations, and an H-Index of 30 according to Google Scholar. He was a co-recipient of the 2014 IEEE Distinguished Contributions to Satellite Communications Award, the CROWNCOM 2015 Best Paper Award, and the 2018 EURASIC JWCN Best Paper Award.

FRANK ZIMMER received the Dipl.Ing. (FH) degree in electrical engineering from the University of Applied Sciences, Kaiserslautern, Germany, and the D.E.A. Diploma degree in signal theory and communications from the University of Vigo, Spain.

He is currently a Senior Manager with SES S.A., where he is also the Head of the Systems Engineering Section. His research interests include autonomous agents and multiagent systems, embedded systems, the IoT, software radio technologies, and systems engineering. He is a member of the ACM and INCOSE.